J. Anat. (2004) **204**, pp123–131

Microvascularization of the human digit as studied by corrosion casting

S. Sangiorgi,[1] A. Manelli,[2] T. Congiu,[1] A. Bini,[2] G. Pilato,[2] M. Reguzzoni[1] and M. Raspanti[1]

[1]*Department of Human Morphology, Laboratory of Human Morphology L.Cattaneo, and* [2]*Department of Orthopedic and Traumatologic Sciences, University of Insubria, Varese, Italy*

Abstract

The aim of this study was to describe microcirculation in the human digit, focusing on the vascular patterns of its cutaneous and subcutaneous areas. We injected a functional supranumerary human thumb (Wassel type IV) with a low-viscosity acrylic resin through its digital artery. The tissues around the vessels were then digested in hot alkali and the resulting casts treated for scanning electron microscopy. We concentrated on six different areas: the palmar and dorsal side of the skin, the eponychium, the perionychium, the nail bed and the nail root. On the palmar side, many vascular villi were evident: these capillaries followed the arrangement of the fingerprint lines, whereas on the dorsal side they were scattered irregularly inside the dermal papillae. In the hypodermal layer of the palmar area, vascular supports of sweat glands and many arteriovenous anastomoses were visible, along with glomerular-shaped vessels involved in thermic regulation and tactile function. In the eponychium and perionychium, the vascular villi followed the direction of nail growth. In the face of the eponychium in contact with the nail, a wide-mesh net of capillaries was evident. In the nail bed, the vessels were arranged in many longitudinal trabeculae parallel to the major axis of the digit. In the root of the nail, we found many columnar vessels characterized by multiple angiogenic buttons on their surface.

Key words corrosion casting technique; human digit; scanning electron microscope.

Introduction

When we think of 'visible microcirculation', we tend to visualize the extremities, in particular the digits. They occupy a very small part of the whole body, but are considered to be the finest window on the internal environment, second only to the eyes.

In fact, such a small environment encapsulates many of the major functions of the body: the tactile, stereognosic and thermal activities.

The high specialization of the structures involved is represented by the wide range of vascular patterns, detectable only by in-depth three-dimensional (3D) analysis of their spatial arrangement and their relationship with the cellular environment (Conrad, 1971).

Correspondence
Dr Simone Sangiorgi, Laboratory of Human Morphology, Via Monte Generoso 71, 21100 Varese, Italy. T: +39 0332264847; F: +39 0332263324; E: simo.med@libero.it

Accepted for publication *15 October 2003*

The corrosion casting technique seemed the best method to investigate the vascular network of the digit in its deepest 3D features; we have been able to describe not only different structural conformations but also subtle ultrastructural detail (Murakami, 1971; Hodde & Nowell, 1980; Lametschwandtner et al. 1990).

This technique consists of a precasting treatment used to clean the vascular lumen and remove the blood, followed by injection of the casting medium (Weiger et al. 1986), a corrosive treatment to macerate all organic components, dissection, mounting, coating and observation by scanning electron microscopy (SEM).

This method provides a snapshot of the microcirculation in the finger, giving clear proof of each structure reached by a vascular support (Hundeiker, 1971).

Applied to deep finger microcirculation, this technique could explain the wide range of modifications occurring in pathological conditions such as Raynaud's syndrome, ischaemic events, arteriovenous malformations (AVM) (De Takats, 1932), clubbing, thromboangiitis obliterans and modifications in the structure

and conformation of the nail (Roth, 1967; Baden, 1970; Achten & Parent, 1983).

Little is known about the vascular support of the dermal corpuscle from a 3D point of view; our SEM analysis of corrosion casts may go some way to filling this gap. As far as we are aware there is no detailed study of the vascular architecture of the nail root in the literature, even though it represents an important anatomical site of continuous regenerative processes and tissue turnover. Therefore, this study aimed to trace a detailed map of the vessels that build up the microcirculation of the human digit.

Materials and methods

A supranumerary human thumb was explanted from the hand of an 18-year-old male on request. Radiodiagnostic investigation revealed that the digit was composed of two separated phalanxes with a diatrosic articulation between them. For this reason it was classified as Wassel IV type of supranumerary digit.

There was no growing cartilage or signs of osteogenesis. Five minutes after amputation, a neurovascular peduncle of the digit was exposed under a dissection light microscope (WILD M3C, Leica) and shortly afterwards a 24G cannula was inserted in the digital artery. The cannula, attached to the vessel by ligature, was connected to a three-way system.

The first step of the corrosion casting technique consisted of a precasting treatment. We injected 5 mL of heparinized solution to prevent blood from clotting. The pressure of injection was monitored manually paying particular attention not to cause any interstitial oedema. A second injection of 5 mL of saline solution was necessary to remove all the blood and to wash out the heparin from the vascular bed.

We proceeded with fixation of the vascular bed with 5 mL of Karnovsky solution (0.25% glutaraldehyde and 0.25% paraformaldehyde in 0.1 M Na-cacodylate buffer at pH = 7.2) to prevent leakage of the resin and to reduce modifications occurring during injection of the resin into the endothelial cells. The resin (5 mL of MERCOX and 0.2 mL of benzoyl peroxide) was then injected through the cannula with an increased pressure because of its viscosity, until reflux from the venous vessel became evident.

After partial polymerization of the resin (30 min), the finger was dipped in a water bath (60 °C) to complete the hardening process (2 h). The finger then underwent a digestion process in several baths of potassium hydroxide (15%), changed every 12 h at room temperature for 4–5 days. Decalcification of the two phalanxes was obtained using hydrochloric acid (3%). The cast, cleared from tissues, was dissected under a dissection microscope (WILD M3C, Leica) to obtain ten small specimens of six different cutaneous areas before the SEM preparation procedure: two specimens, one transversally and the other longitudinally sectioned, from the palmar side; two specimens from the dorsal side, one specimen of the eponychium (observed twice: first to reveal its cutaneous surface and then, mounted reversed, to reveal its inferior surface, closest to the nail); one specimen of the peryonychium; two specimens of the nail bed and two of the nail root.

The resulting casts were rinsed in distilled water (to prevent deposition of KOH or HCl salt), dehydrated in graded alcohol, critical-point-dried in an Emitech K850 CPD apparatus and mounted on adhesive films applied on aluminium stubs.

In two cases, owing to the size of the cast, we used metallic bridges to make all the specimens conductive.

We coated the casts with 10-nm gold in an Emitech K250 sputter-coater and observed them under a Philips XL-30 FEG SEM operating at 10–15 kV.

Results

The schematic diagram in Fig. 1 gives an overall view of all six areas studied: arrows are used to connect each area of the digit to the micrographs shown later: palmar and dorsal side of digital skin (on the dorsal side

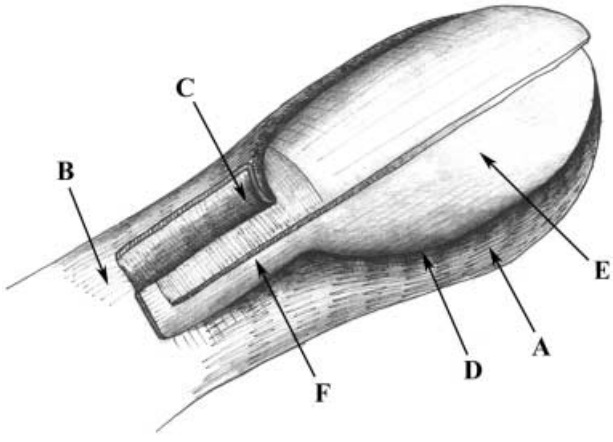

Fig. 1 Schematic representation of the digit in all six areas investigated: palmar (A) and dorsal (B) side of digital skin, eponychium (C), perionychium (D), nail bed (E) and nail root (F): the arrows connect each area to the studied region.

we studied the skin area just before the eponychium), eponychium, perionychium, nail bed and nail root.

Palmar and dorsal side of digital skin

In a transverse section of the skin, on the palmar side, we could distinguish four different vascular layers: the papillary layer with capillaries organized in row-like structures, the subpapillary layer with medium-sized vessels, the reticular layer with large vessels distinguished in arterioles and high endothelial venules, and the hypodermal layer with many capillaries organized in glomerular structures supplying sweat glands and thermoreceptorial systems (Fig. 2).

The vessels of the papillary layer followed the disposition of the lines of the fingerprint (Fig. 3A); for each

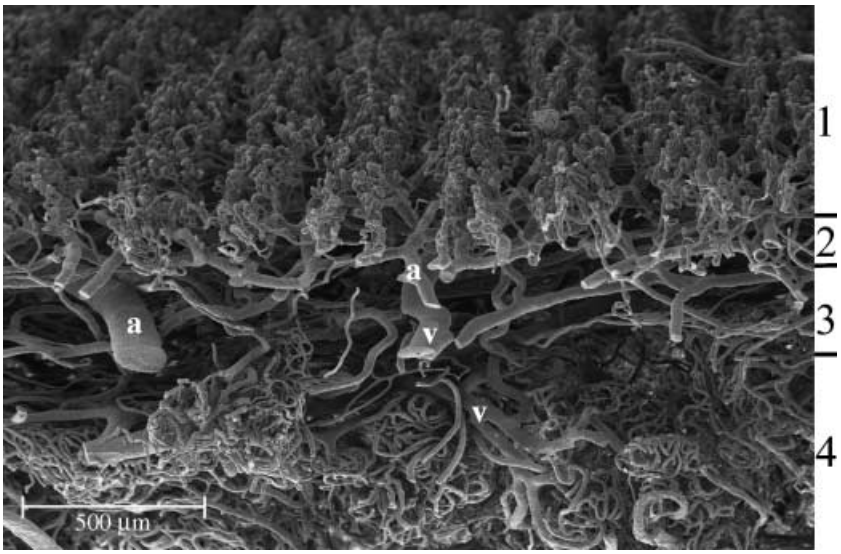

Fig. 2 Palmar side. In transverse section we can distinguish four vascular layers: (1) the papillary layer, (2) the subpapillary layer, (3) the reticular layer and (4) the hypodermal layer: note the glomerular structures supplying sweat glands and thermoreceptorial systems. We can also distinguish the arterial (A) from venular (V) vessels.

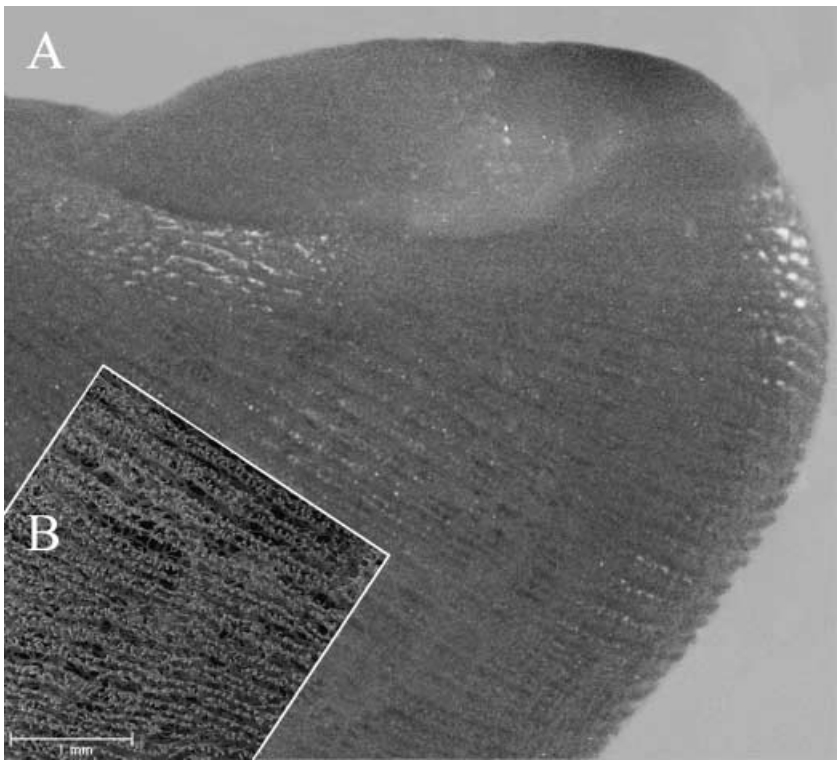

Fig. 3 Palmar side. The digit is seen during the maceration process on the 2nd day of KOH immersion. It already shows the regular linear disposition of vessels along the fingerprints (A); (B) superimposition of an SEM image of the same area, revealing perfect correspondence.

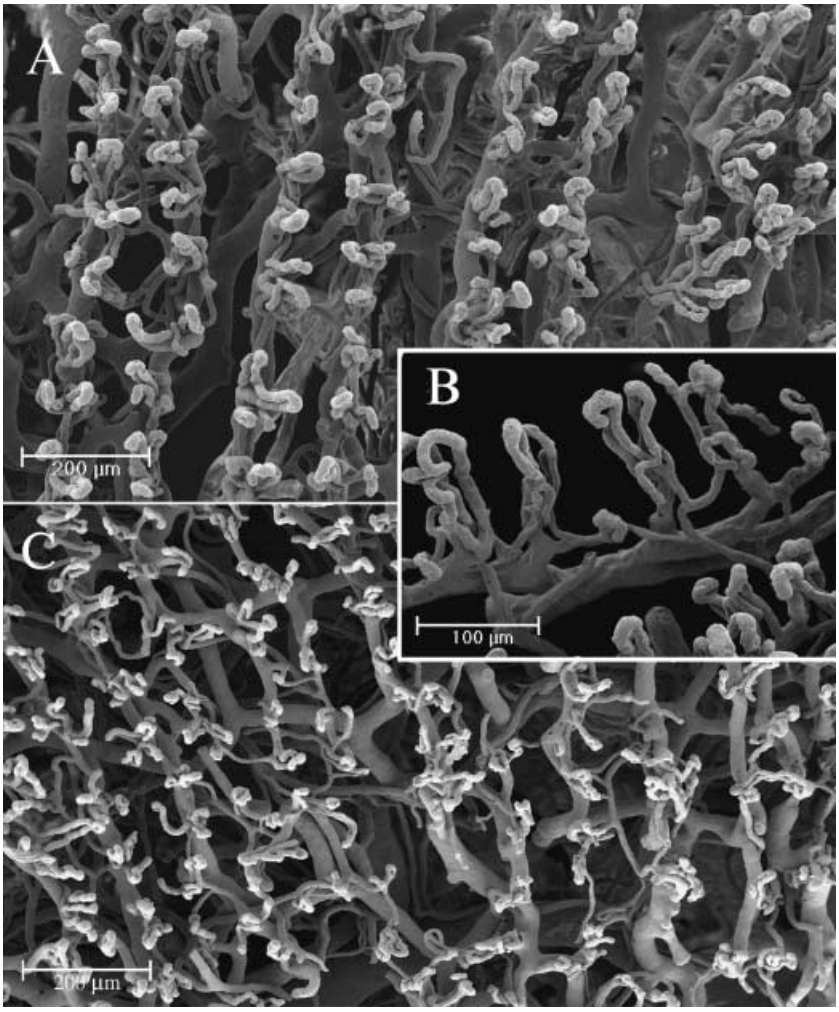

Fig. 4 Palmar and dorsal side. In the palmar side we can observe two rows of vessels following the patterning the fingerprint. (A) The villi that arise from these vessels are 100 μm high and have a dextrogyrate rotation: the distance between each is about 70 μm (B). On the dorsal side the vessels do not follow any pattern (C).

of these, at low magnification, we could clearly see two rows of vessels (Fig. 3B). At high magnification they were spaced about 200 μm apart (Fig. 4A).

From these vessels arose many microvascular villi that penetrated the dermal papillae. These villi were 100 μm high and had a constant dextrogyrate rotation. The distance between each was constant at about 70 μm (Fig. 4B).

In the papillary layer of the dorsal side, the distance between the microvascular villi was extremely variable, ranging from 70 to 180 μm.

In the subpapillary layer of the dorsal side, the vessels lacked the regularity observed on the palmar side, forming a wide net from which other vascular villi with the same dextrogyrate orientation arose (Fig. 4C).

In the hypodermal layer of the palmar side, the blood vessels formed many more specialized structures: the vascular net around the sweat glands, the capillaries around thermoreceptorial corpuscles and cutaneous sensory receptors and many glomic corpuscles for thermic regulation (Fig. 5).

Around the sweat glands, the capillaries formed a tubular-shaped structure comprising two parts, the first feeding the body of the gland and the other supplying the excretory duct (Fig. 5A).

The vascularization of sensory receptors was represented by a glomerular conic structure adapted to the convexity of dermal papillae, where these systems are usually found (Fig. 5B).

We often found arteriovenous anastomoses in the dermal layer, in the form of either a glomerular-shaped body or a direct connection. On the surface of the cast, shallow impressions of various shapes and sizes corresponded to the nuclei of endothelial cells (Fig. 5C).

Eponychium

In the eponychium, the angle formed between the axis of the vascular villi on the dorsal side of the skin and the major axis of the digit progressively diminished

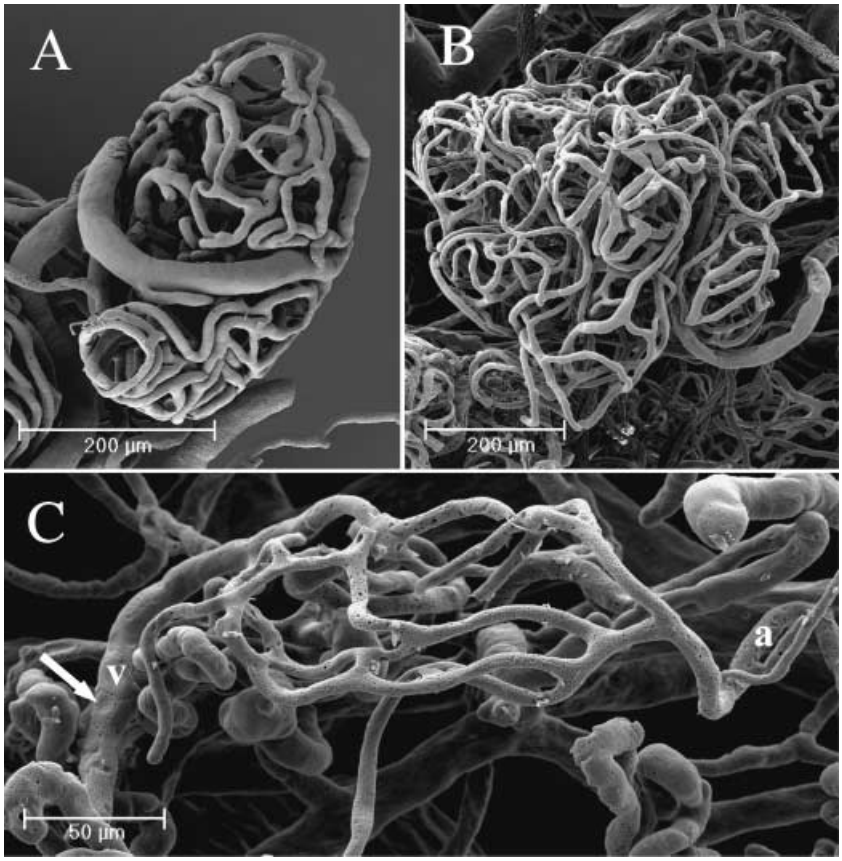

Fig. 5 Palmar side. In the hypodermal layer of the palmar side, we can observe many glomeruloid vascular structures: the vessels supplying the sweat glands (A), the capillaries surrounding thermoreceptorial corpuscles (B) and some glomic bodies or arteriovenous anastomoses (C). In the glomic body, we can distinguish the artery (a) from the vein (v) by looking at the nuclear impressions left on the cast by the endothelial cells (thin arrow).

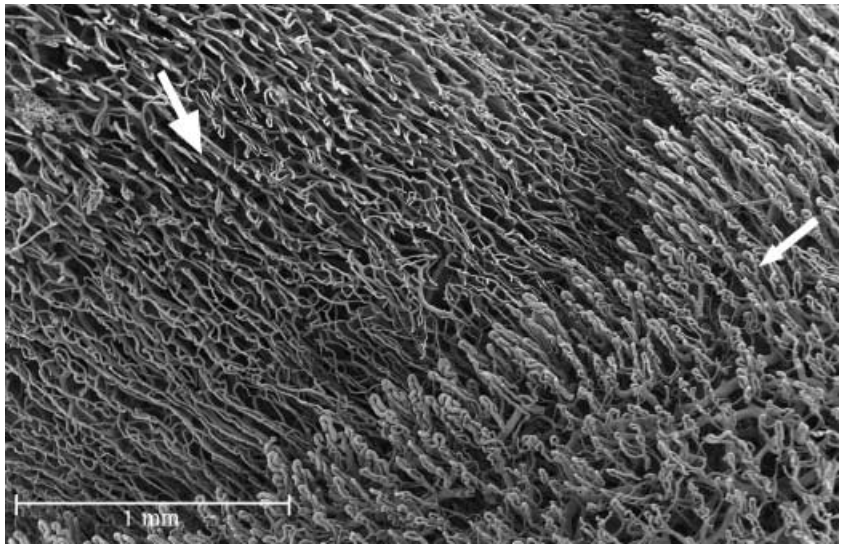

Fig. 6 Eponychium. The angle formed between the axis of the vascular villi on the dorsal side of the skin and the major axis of the digit progressively diminishes towards the eponychium (thin arrow) – nail (thick arrow) border.

to the eponychium–nail border, whereas their height increased, following the shape of the dermal papillae located in that region (Fig. 6).

On the surface of the eponychium in contact with the nail, both the arterial and venular vessels had a regular net-like concave disposition that followed the shape of the nail (Fig. 7A). This net ended in correspondence with the passage to the cutaneous surface of the eponychium, giving rise to a number of long capillary loops penetrating the dermal papillae and orientated along the major axis of the nail (Fig. 7B).

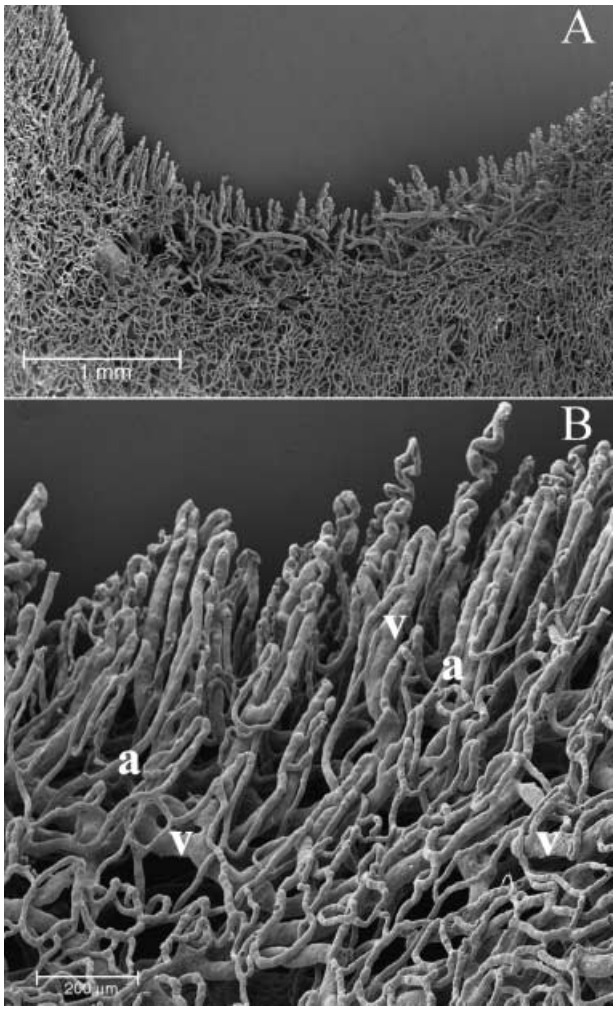

Fig. 7 Eponychium. At lower magnification we can clearly see the convexity of the face in contact with the nail (A). At high magnification we can distinguish a regular vascular net that gives rise to the first long vascular villi of the eponychium (B). We can distinguish the artery (a) from the vein (v) by their different morphological conformation.

Perionychium

In the perionychium, the capillaries seemed to be stretched by the force of nail growth: they formed an irregular net of compressed capillaries extending from the cutaneous part of the perionychium to the nail bed (Fig. 8).

Nail bed

In the nail bed, the vessels began to form a number of loops, longitudinally orientated along the major axis of the nail (Fig. 9A). Each loop had a gradual longitudinal inclination, as a result of the natural growing motion of the nail, to the fingertip where these ridges became the vascular villi of the palmar side of the finger. These loops also had a gradual coronal inclination, from the centre of the nail bed to the perionychium (Fig. 9B).

Nail root

In the nail root, the vessels, mostly arterioles, were orientated longitudinally along the major axis of the finger (Fig. 10A). These vessels originated in a spiral shape, and gradually straightened (Fig. 10B).

In this area, a number of neoangiogenic buttons were evident on the arterial vessels, showing several 3D patterns usually found in highly regenerating or tumoral tissues: dome-shaped elevations, small flaps or formation of collaterals (Fig. 11A–C). The neoangiogenic formations ended at the passage from nail root to nail bed, when the nail was no longer covered by the eponychium.

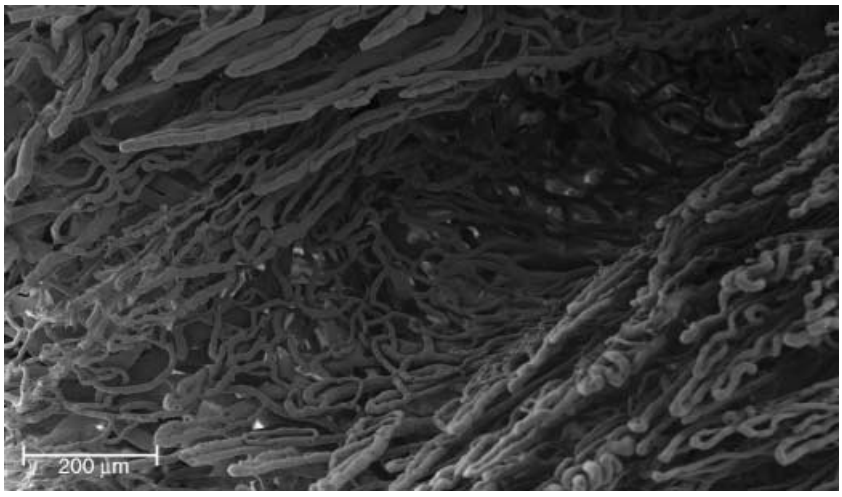

Fig. 8 Perionychium. The passage from the nail bed to the peryonichium is made up of an interlaced net of thin vessels, where the pressure of the nail on the tissue is higher, going from the trabecular area of the nail bed to the vascular villi of the skin region.

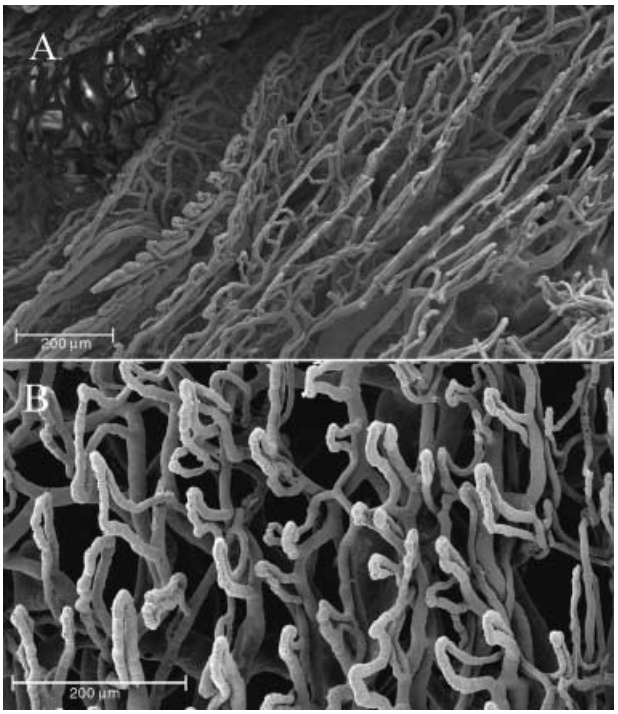

Fig. 9 Nail bed. Two different patterns of disposition of vascular trabeculae: the vessels begin to form a number of loops, longitudinally orientated along the major axis of the nail to the passage to the eponychium (A). The vascular loops have a gradual coronal inclination in the middle of the nail bed (B).

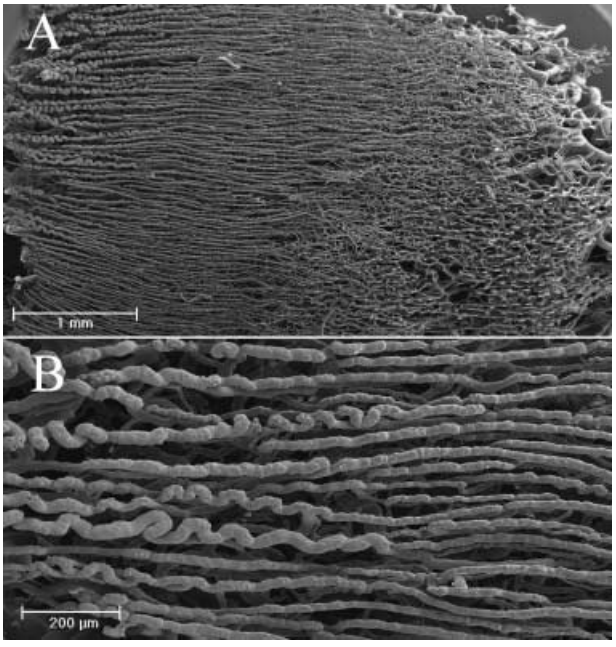

Fig. 10 Nail root. The vascular architecture is composed of an area with helicoidal-shaped vessels that gradually turn into longitudinal vessels, giving rise to the trabeculae of the nail bed (A). These vessels are spiral-shaped when they originate, and gradually straighten (B).

Discussion

The corrosion casting method, combined with SEM investigation, gives an accurate 3D representation of microvascular architecture in human digital skin. This technique enhances the subtle differences existing between the disposition and organization of medium-sized vessels and capillaries either in superficial or in deeper digital areas (Edwards, 1960; Backhouse, 1981; Moss & Schwartz, 1985).

Even if some artefacts are encountered, corrosion casting represents the most valid device for obtaining a deep morphological 3D description of these different vascular architectures. Applied to the human digit, the resin casts proved not only useful for scientific purposes, but also as a complete teaching device.

Thanks to their three-dimensionality and defined shape, the casts are easily interpretable, in structural as well as in ultrastructural details.

We focused our attention on different cutaneous vascular patterns trying to relate them to a morpho-functionally well-defined area. In a transverse section of the skin, we could easily distinguish the four vascular layers described: the papillary layer, the closest to the external environment and probably the most specialized, was made up of many vascular villi formed by an afferent ascending vessel and an efferent descending one (Pollit & Molyneux, 1990; Nasu et al. 1998).

On the palmar side of the human digit, we observed the regular disposition of capillaries that sharply followed the cutaneous sulci of the fingerprint, reproducing an identical 'vascular fingerprint' with the same individual architecture of the cutaneous area (Hale, 1951; Miyamoto, 1963; Blanka & Alter, 1976).

With their architectural features, they followed the sharp arrangement and shape of the dermal papillae. Their differences in structure and size depend on the functional and anatomical characteristics of the site supplied (Misumi & Akiyoshi, 1984; Kawabe et al. 1985).

This variability has also been observed in vascular injury and during the regeneration process when vessels lose their original shape because of scar formation (Selliseth & Selvig, 1995).

The vessels in the subpapillary and reticular layers form a closely interlaced net, necessary for sustaining and maintaining the elasticity of the upper layer. The hypodermal layer (Straile, 1969), the fourth on the palmar side, is made up of many microvascular units: some of these feed the thermoregulatory systems and

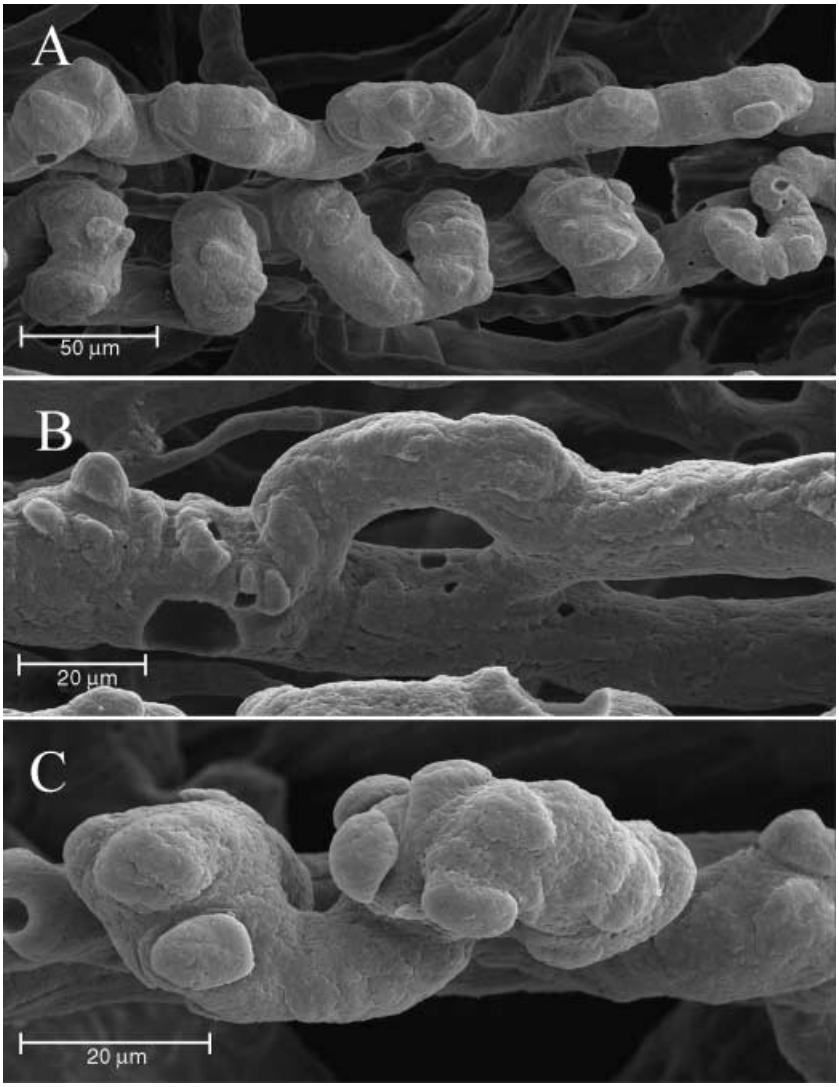

Fig. 11 Nail root. On the helicoidal vessels found in the nail root a number of angiogenic buttons are visible (A). At high magnification, we can distinguish different patterns of conformation: formation of collaterals (B) and dome-shaped elevations (C).

many sensory receptors whereas others supply the sweat glands (Bryce & Chizuka, 1988). The fingertip is full of these flake-like structures: a clear demonstration of the tactile and thermoregulatory functions of this area. The concentration of these structures decreases from the palmar to the dorsal side of the finger.

The thermic environmental variations and the physiological lower temperature of the extremities require several thermoregulatory systems that are mostly found in the glomic bodies and arteriovenous shunts (Grant & Bland, 1930). Glomic bodies, glomerular structures of tortuous thin vessels are involved in many pathological conditions as well as representing the first corpuscle that alerts the body to an excessive variation in environmental temperature.

These systems take an active part in the pathophysiology of Raynaud's syndrome and in many thermic vasospastic phenomena. Moreover, the obstruction of these capillaries as a result of vasculitic, septic or traumatic events can lead to the classic paresthesic symptoms in the extremities.

In all these layers, we can distinguish the arterial from the venular vessels using several parameters: the shape of the transverse section of the cast (circular in arterial vessels and elliptical in venular vessels) and the disposition of the impression of nuclei and junction of endothelial cells on the cast. The nuclear impressions appear ovoid in arterial vessels and circular in venular vessels. The imprints of endothelial cell junctions are elongated and arranged along the major axis of the vessel in arteries, whereas in veins they appear polygonal and irregular.

In the eponychium, the distribution of capillary loops follows the sharp orientation of dermal papillae, dragged

proximal to distal by growth of the nail. In the perionychium, the high pressure exerted by the nail stretches the capillaries, forming an irregular vascular net. In the nail bed, the capillary loops strictly follow the two directions of nail growth: longitudinal and coronal. The loops have a gradual longitudinal inclination from nail root to fingertip, and a transverse inclination from the centre to the perionychium.

One of the most impressive findings was the clear diffusion of angiogenic buttons in the nail root, probably as a result of the nail regenerating process already reported in pathological conditions (Miodonski et al. 1980; Tano et al. 1981; Grunt, 1992; Rolf & Nilsson, 1992). This fact can be explained by the high degree of cell turnover in this region.

Our study revealed some 3D features of the human digit, as observed from a microvascular point of view. We focused on the strict connection existing between the physiological mechanisms of this 'organ' and its specialized vessels.

This research is ongoing and we plan to extend the study to the investigation of the disposition of lymphatics usually implicated in the formation of oedema (Castenholz, 1989).

References

Achten G, Parent D (1983) The normal and pathologic nail. *Int. J. Dermatol.* **22**, 556–565.

Backhouse KM (1981) The blood supply of the arm and hand. In *The Hand* (ed. Saunders WB), pp. 297–309. Philadelphia: Tubiana R.

Baden HP (1970) The physical properties of nail. *J. Invest. Dermatol.* **55**, 115–122.

Blanka S, Alter M (1976) *Dermatoglyphics in Medical Disorders*. New York: Springer-Verlag.

Bryce LM, Chizuka IDE (1988) The structure and function of cutaneous sensory receptors. *Arch. Histol.* **51**, 1–34.

Castenholz A (1989) Interpretation of structural patterns appearing on corrosion casts of small blood and initial lymphatic vessels. *Scann. Microsc.* **3**, 315–325.

Conrad MC (1971) Role of the circulation of the skin in maintaining normal body temperature. In *Functional Anatomy of the Circulation to the Lower Extremities*, pp. 115–131. Chicago: Year Book Medical Publishers.

De Takats G (1932) Vascular anomalies of the extremities. Report of five cases. *Surg. Gynecol. Obstet.* **55**, 227–237.

Edwards EA (1960) Organization of the small arteries of the hand and digits. *Am. J. Surg.* **99**, 837–846.

Grant RT, Bland EF (1930) Observations on arteriovenous anastomoses in human skin and in the bird's foot with special reference to cold. *Heart* **15**, 385–411.

Grunt TW (1992) The Fundamental vascular structures in epithelial cancer demonstrated in an experimental lung carcinoma. In *Scanning Electron Microscopy of Vascular Casts: Methods and Applications* (eds Motta PM, Murakami T), pp. 331–344. Amsterdam: Kluwer Academic Publishers.

Hale AR (1952) Morphogenesis of volar skin in the human fetus *Am. J. Anat.* **91**, 147–157.

Hodde KC, Nowell JA (1980) SEM of micro-corrosion casts. *Scann. Electron. Microsc.* **II**, 88–106.

Hundeiker M (1971) Hautrelief und Capillararchitektur. *Arch. Derm. Forsch.* **242**, 78–86.

Kawabe TT, MacCallum DK, Lillie JH (1985) Variation in basement membrane topography in human thick skin. *Anat. Rec.* **211**, 142–148.

Lametschwandtner A, Lametschwandtner U, Weiger T (1990) Scanning electron microscopy of vascular corrosion casts – technique and applications. *Updated Scann. Microsc. Rev.* **4**, 889–941.

Miodonski A, Kus J, Olszewski E, Tyrankiewicz R (1980) Scanning electron microscopic studies on blood vessels in cancer of the larynx. *Arch. Otolaryngol.* **106**, 321–332.

Misumi Y, Akiyoshi T (1984) Scanning electron microscopic structure of the finger print as related to the dermal surface. *Anat. Rec.* **208**, 49–55.

Miyamoto Y (1963) *Fingerprints*. Tokyo: Japan Publications Co.

Moss SH, Schwartz KS (1985) Digital venous anatomy. *J. Hand. Surg.* **10**, 473–482.

Murakami T (1971) Application of the scanning electron microscope to the study of the fine distribution of blood vessels. *Arch. Histol. Jpn* **32**, 445–454.

Nasu T, Yamanaka T, Nakai M, Ogawa H (1998) Scanning electron microscopic study of the vascular supply of the equine hoof. *J. Vet. Med. Sci.* **60**, 855–858.

Pollitt CC, Molyneux GS (1990) A scanning electron microscopical study of the dermal microcirculation in the equine foot. *Equine Vet. J.* **22**, 79–87.

Rolf HC, Nilsson BO (1992) *Microvascular Corrosion Casting in Angiogenesis Research in Scanning Electron Microscopy of Vascular Casts: Methods and Applications*. Amsterdam: Kluwer Academic Publishers.

Roth SI (1967) Hair and nail. In *Ultrastructure of Normal and Abnormal Skin* (ed. Zelickson AS), pp. 105–131. Philadelphia: Lea & Febiger.

Selliseth NJ, Selvig KA (1995) Revascularization of an excisional wound in gingival and oral mucosa. A scanning electron microscopic study using corrosion casts in rats. *Scanning Microsc.* **9**, 455–467.

Straile WE (1969) Vertical cutaneous organization. *J. Theor. Biol.* **24**, 203–215.

Tano Y, Chandler DB, Machemer R (1981) Vascular casts of experimental retinal neovascularization. *Am. J. Ophthalmol.* **92**, 110–120.

Weiger T, Lametschwandtner A, Stockmayer P (1986) Technical parameters of plastics (Mercox CL-2B and various methylmethacrylates) used in scanning electron microscopy of vascular corrosion casts. *Scann. Electron. Microsc.* **I**, 243–252.